

Original Article
Cardiovascular Disorders



Surgically Metabolic Resection of Pericardial Fat to Ameliorate Myocardial Mitochondrial Dysfunction in Acute Myocardial Infarction Obese Rats

Ki-Woon Kang ,^{1*} Ju-Young Ko ,^{2*} Hyunghee Lee ,¹ Seung Yong Shin ,¹ Wang Soo Lee ,¹ Joonhwa Hong ,³ Sang-Wook Kim ,¹ Seong-Kyu Lee ,⁴ and Min-Ho Oak ²



Received: Nov 7, 2021
Accepted: Jan 24, 2022
Published online: Feb 8, 2022

Address for Correspondence:

Ki-Woon Kang, MD, PhD
Division of Cardiology, College of Medicine,
Heart Research Institute and Biomedical
Research Institute, Chung-Ang University
Hospital, Chung-Ang University 102 Heukseok-
ro, Dongjak-gu, Seoul 06973, Republic of
Korea.
Email: kwkang0115@gamil.com

Min-Ho Oak, PhD
College of Pharmacy, Mokpo National
University, 1666 Yeongsan-ro, Cheonggye-
myeon, Muan 58554, Republic of Korea.
Email: mhoak@mokpo.ac.kr

*Ki-Woon Kang and Ju-Young Ko equally
contributed to this manuscript.

© 2022 The Korean Academy of Medical
Sciences.
This is an Open Access article distributed
under the terms of the Creative Commons
Attribution Non-Commercial License (<https://creativecommons.org/licenses/by-nc/4.0/>)
which permits unrestricted non-commercial
use, distribution, and reproduction in any
medium, provided the original work is properly
cited.

ORCID iDs

Ki-Woon Kang
<https://orcid.org/0000-0002-1361-0022>
Ju-Young Ko
<https://orcid.org/0000-0002-8171-3832>

¹Division of Cardiology, College of Medicine, Heart Research Institute and Biomedical Research Institute, Chung-Ang University Hospital, Chung-Ang University, Seoul, Korea
²College of Pharmacy, Mokpo National University, Muan, Korea
³Division of Cardiothoracic Surgery, College of Medicine, Chung-Ang University Hospital, Chung-Ang University, Seoul, Korea
⁴Department of Biochemistry and Molecular Biology, School of Medicine, Eulji University, Daejeon, Korea

ABSTRACT

Background: Pericardial fat (PF) is highly associated with cardiovascular disease but the effectiveness of surgical resection of PF is still unknown for myocardial mitochondrial structure and function in acute myocardial infarction (AMI) with obesity. The aim of this study was to demonstrate the difference in myocardial mitochondrial structure and function between obese AMI with additionally resected PF and those without resected PF.

Methods: Obese rats with 12-week high fat diet (45 kcal% fat, n = 21) were randomly assigned into 3 groups: obese control, obese AMI and obese AMI with additionally resected PF. One week after developing AMI and additional resection of PF, echocardiogram, myocardial mitochondrial histomorphology, oxidative phosphorylation system (OXPHOS), anti-oxidative enzyme and sarcoplasmic reticulum Ca²⁺ ATPase 2 (SERCA2) in the non-infarcted area were assessed between these groups.

Results: There was significant improvement of systolic function in AMI with PF resection compared with the AMI group in the echocardiogram. Even though the electron microscopic morphology for the mitochondria seems to be similar between the AMI with PF resection and AMI groups, there was an improved expression of PGC-1 α and responsive OXPHOS including NDUFB3, NDUFB5 and SDHB are associated with the ATP levels in the AMI with PF resection compared with those in the AMI group. In addition, the expression levels of antioxidant enzymes (MnSOD) and SERCA2 were improved in the AMI with PF resection compared with those in the AMI group.

Conclusion: Surgical resection of PF might ameliorate myocardial mitochondria dysfunction in obese AMI.

Keywords: Acute Myocardial Infarction; Heart Failure; Pericardial Fat; Surgical Resection

Hyunghee Lee <https://orcid.org/0000-0002-9208-3493>Seung Yong Shin <https://orcid.org/0000-0002-3408-6899>Wang Soo Lee <https://orcid.org/0000-0002-8264-0866>Joonhwa Hong <https://orcid.org/0000-0003-2212-2861>Sang-Wook Kim <https://orcid.org/0000-0002-7208-8596>Seong-Kyu Lee <https://orcid.org/0000-0002-5999-7656>Min-Ho Oak <https://orcid.org/0000-0001-5584-1702>**Funding**

This study was supported by a research grant from the National Research Foundation of Korea funded by the Ministry of Education (2020R111A3A04037859), partly by a research grant from Biomedical Research Institute, Chung-Ang University Hospital (2021) and partly by Samjin Pharm. Co., Ltd. (SJ-IIT-22-11).

Disclosure

The authors have no potential conflicts of interest to disclose.

Author Contributions

Conceptualization: Kang KW. Data curation: Kang KW, Lee H, Lee SK. Formal analysis: Kang KW, Ko JY, Lee H, Lee SK. Funding acquisition: Kang KW. Methodology: Kang KW, Ko JY, Lee H, Shin SY, Lee WS, Hong J, Kim SW. Writing - original draft: Kang KW, Ko JY, Lee H, Shin SY, Lee WS, Hong J, Kim SW, Lee SK, Oak MH. Writing - review & editing: Kang KW, Oak MH.

INTRODUCTION

Cardiovascular disorders are the leading cause of death representing all global deaths¹ and acute myocardial infarction (AMI) is a common cause of cardiovascular disorders.² Ischemia with inflammation in the cardiomyocyte is the main pathophysiology of AMI.³ In addition, obesity is strongly associated with an increased risk of developing AMI or heart failure.^{4,5} Especially, pericardial fat (PF) has been shown to have a diverse role⁶ in locations not classically associated with adipose tissue storage,⁷ but with the occurrence of cardiovascular events.⁸ A large amount of PF has been known to be significantly associated with cardiovascular diseases,²⁻⁵ and decrease anti-inflammatory adiponectin production and increase the synthesis of pro-inflammatory adipokines in obesity.⁶ In response to AMI, mesenchymal cells from the PF could migrate into the myocardium to be transformed into fibroblasts^{7,8} and shift to a nidus for inflammation and oxidative stress subsequent to aggravating cardiovascular disease,^{7,8} which demonstrates the paracrine effect of PF as a pathological transformation for cardiac damage and dysfunction. A recent study demonstrated that surgically resected PF improved the inflammatory status.⁹⁻¹¹ In addition, mitochondrial oxidative phosphorylation system (OXPHOS) and adenosine triphosphate (ATP) in the cardiomyocyte were mainly suppressed in the animal with cardiac dysfunction^{12,13} and PGC-1 α with oxidative stress was also significantly associated with heart failure.¹⁴⁻¹⁶

Therefore, we investigated whether surgical resection of PF ameliorates myocardial mitochondrial structure, and dysfunction in the AMI obese rat model.

METHODS**Rats and housing**

Animal female Wistar rats (6 weeks old, 160 g) were purchased from Harlan (Madison, WI, USA) and housed in the Animal Care Center of Eulji University in Daejeon under controlled conditions. The rats were housed in pairs at $23 \pm 1^\circ\text{C}$ with a 12 hours light/dark cycle and given access to water and rat chow consisting of a 'high fat diet (HFD)' (45% calories from fat).

Study design

After 12 weeks of HFD, all rats ($n = 21$) were randomly assigned into 3 groups: control, AMI, and AMI with PF resection. Subjects were anesthetized with 10% chloral hydrate by peritoneal injection and ventilated with a rodent respirator. The chest was opened through the left thoracotomy so that the left anterior descending coronary could be visualized and permanently ligated with a 7-0 silk suture at the site of its emergence from the left ventricle or so that a sham operation could be performed without ligation as described previously.¹⁵ The control group ($n = 7$) had the sham operation among the rats ($n = 14$) who had a permanent ligation of the left anterior descending artery, the AMI with PF resection group ($n = 7$) had an additional PF resection (**Supplementary Fig. 1**). In the AMI with PF resection group, the PF covering the anterior aspect of the heart was removed during the AMI operation.

Sampling, histology and transmission electron microscopy (TEM)

The blood samples and myocardial tissues of all rats were collected after the echocardiogram and sacrifice. Serum was stored at -80°C until further analyses, and myocardial tissues were snap-frozen and stored at -80°C , and some of the non-infarct myocardial tissues were fixed for

histologic examination or TEM. Transverse sections in each group were fixed in 10% buffered formalin (Sigma Aldrich, Co., St Louis, MO, USA) and embedded in paraffin. Thick transverse sections of 1 μ m were cut from the tissue block and stained with hematoxylin and eosin,¹⁷ and myocardial tissues were fixed in 2.5% paraformaldehyde-glutaraldehyde at 4°C for 24 hours and then washed with 0.1 M phosphate buffered solution at 4°C. After washing two times, the tissue was post-fixed with 1% OsO₄ buffered solution (pH 7.4) for 1 hour and 30 minutes. Tissue samples were dehydrated by serial ethanol and propylene oxide treatment and embedded in Poly/EM Bed812 embedding medium, and the resin was then polymerized in a vacuum drying oven (Yamato Scientific, Tokyo, Japan) at 60°C for 48 hours. Non-infarct myocardial tissue was sectioned using an EM Ultra-microtome LKB-2088 and stained with 1% toluidine blue, and then, ultra-thin sections were double-stained with uranyl acetate and lead citrate and examined using a Hitachi H-7600 electron microscope (Hitachi, Tokyo, Japan).

Echocardiogram

An echocardiogram was undertaken one week after the AMI operation as described previously.¹⁸ All rats were anesthetized by intraperitoneal injection with a mixture of ketamine (50 mg/kg) and xylazine (1 mg/kg), and the hair of the chest wall of all rats was carefully removed, and warm ultrasound transmission gel was liberally applied to ensure an optimal image quality for the echocardiogram. A high-frequency 15-MHz linear transducer (Entos CL15-7; Philips Medical Systems, Bothell, WA, USA) connected to an ultrasound system (ATL-HDI5000; Philips Medical Systems) was used for the acquisition of echocardiographic images. All cardiac structure and function traces were manually measured with a caliper by an operator using the leading-edge method according to the American Society of Echocardiography.¹⁹

Real time polymerase chain reaction

The acquired myocardial tissue was homogenized using a polytron homogenizer (Fisher Scientific Inc., Pittsburgh, PA, USA), and the homogenate was stored to permit the complete dissociation of nucleoprotein complexes. Homogenates containing 0.2 mL of chloroform per 1 mL of TRI Reagent (Molecular Research Center Inc., Cincinnati, OH, USA) were shaken, and total RNA from the homogenates was isolated according to the manufacturer's instructions, and equal amounts of total RNA were reverse transcribed into cDNA using the iScript cDNA Synthesis Kit (Bio-Rad, Hercules, CA, USA) (The primer sequences are listed in the **Supplementary Table 1**). Real-time polymerase chain reaction was done in a 20 μ L reaction mixture containing 1 μ g cDNA, 10 pmol of forward primer and reverse primer each, and 10 μ L of SYBR Green Supermix (Bio-Rad) using a CFX96 Real-Time PCR Detection System (Bio-Rad Laboratories [Singapore] Pte Ltd., Singapore). The threshold cycle values for each target mRNA were normalized to the mRNA of glyceraldehyde-3-phosphate dehydrogenase (GAPDH), and the relative expression level of each target gene was calculated using the CFX Manager software version 1.5 (Bio-Rad).

Western blot analysis

Acquired myocardial tissues were homogenized in the Pro-Prep Protein Extraction Solution (Intron Biotechnology, Seoul, Korea) with protease inhibitor (Roche Applied Science, Penzberg, Germany) and phosphatase inhibitor (Roche Applied Science). All the homogenates were incubated overall for 30 minutes and centrifuged at 13,000 rpm (4°C) for 5 minutes, and the supernatant was transferred into a 1.5 ml tube. Lysates were run on a 4–20% MP TGX Precast Gel (Bio-Rad) and transferred to PVDF membranes using a wet, vertical Criterion Blotter (Bio-Rad). Membranes were blocked with 5% skim milk in 50 mmol/L

Tris-HCl (pH 7.4) and 150 mmol/L NaCl (TBS) and then incubated overnight at 4°C with antibodies. The anti-GAPDH antibody (1:1,000) was obtained from Cell Signaling (Beverly, MA, USA), and the NDUFB3, NDUFB5 and SDHB antibodies (1:1,000) were obtained from Novus Biologicals (Littleton, CO, USA).

Antibodies directed against PGC-1 α (1:500) were obtained from Cell Signaling. All antibody dilutions were made in 0.5% bovine serum albumin [BSA] and 0.1% sodium azide-Tris-buffered saline-Tween 20 [TBST], and the membranes were incubated with the appropriate horseradish peroxidase-conjugated secondary antibody. Secondary antibodies (goat anti-rabbit IgG) were obtained from Cell Signaling, and the signal was developed using an enhanced chemiluminescence detection system (Millipore, Billerica, MA, USA).

ATP measurements

The acquired myocardial tissues were homogenized in mammalian cell ATP lysis solution (Perkin-Elmer, Waltham, MA, USA). The whole homogenates were centrifuged at 12,000 rpm (4°C), and the supernatants were transferred into 1.5 mL tubes. Then, the ATPlite assay was performed according to the manufacturer's instructions (Perkin-Elmer), and the luminescence emitted from the ATP-dependent luciferase reaction was calculated using a 2030 Multi-label Reader (Perkin-Elmer).

Statistical analysis

All parameters were expressed as the mean \pm standard deviation and analyzed by one-way analysis of variance with Tukey's post hoc test. Statistical analyses were performed using SPSS (version 15.0; SPSS Inc., Chicago, IL, USA), and a *P* value < 0.05 was considered statistically significant.

Ethics statement

All experiments were approved by the Animal Welfare Committee of Eulji University (EUIACUC19-28) in Daejeon, Republic of Korea.

RESULTS

The comparison of the echocardiographic parameters between AMI and AMI with PF resection

Systolic interventricular septum (IVSs), diastolic interventricular septum (IVSd), and diastolic left ventricular posterior wall (LVPWd) were similar between the AMI with PF resection and AMI groups (Table 1). However, systolic left ventricular intraventricular dimension (LVIDs)

Table 1. The comparison of echocardiographic parameters between groups

Echocardiographic parameters	Control group	AMI group	AMI + PF resection group	<i>P</i> value
LVPWs (cm)	0.15 \pm 0.02	0.12 \pm 0.02	0.12 \pm 0.02	0.999
LVIDs (cm)	0.42 \pm 0.04	0.64 \pm 0.09	0.53 \pm 0.11	0.243
IVSs (cm)	0.14 \pm 0.03	0.12 \pm 0.03	0.11 \pm 0.02	0.536
LVPWd (cm)	0.13 \pm 0.02	0.13 \pm 0.02	0.13 \pm 0.02	0.999
LVIDd (cm)	0.59 \pm 0.07	0.72 \pm 0.11	0.69 \pm 0.12	0.490
IVSd (cm)	0.10 \pm 0.02	0.12 \pm 0.03	0.10 \pm 0.02	0.131

AMI = acute myocardial infarction, PF = pericardial fat, LVPWs = systolic left ventricular posterior wall, LVIDs = systolic left ventricular intraventricular dimension, IVSs = systolic interventricular septum, LVPWd = diastolic left ventricular posterior wall, LVIDd = diastolic left ventricular intraventricular dimension, IVSd = diastolic interventricular septum.

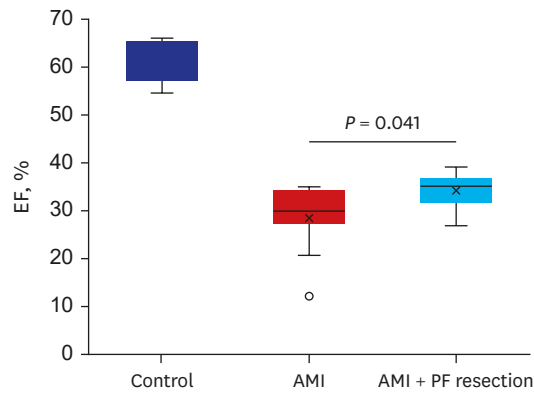


Fig. 1. The comparison of cardiac function between AMI and AMI with PF resection. EF was measured by echocardiography. Values are expressed as mean \pm standard deviation.

AMI = acute myocardial infarction, PF = pericardial fat, EF = ejection fraction.

* $P < 0.05$.

and diastolic left ventricular intraventricular dimension (LVIDd) were slightly decreased in the AMI with PF resection group compared to the AMI group which shows that the left ventricular systolic function was significantly recovered in the AMI with PF resection group compared to the AMI group ($34.3 \pm 3.8\%$ vs. $28.5 \pm 7.3\%$, $P = 0.041$) (**Fig. 1**).

Histomorphology and transmission electron microscopic images of mitochondria in the myocardium

The electron microscopic images of the non-infarct area between the AMI and AMI with PF resection groups seem to be similar at first look (**Fig. 2**). However, the myocardial mitochondria in the AMI with PF resection group showed more electro-dense cristae and membrane than those in the AMI group.

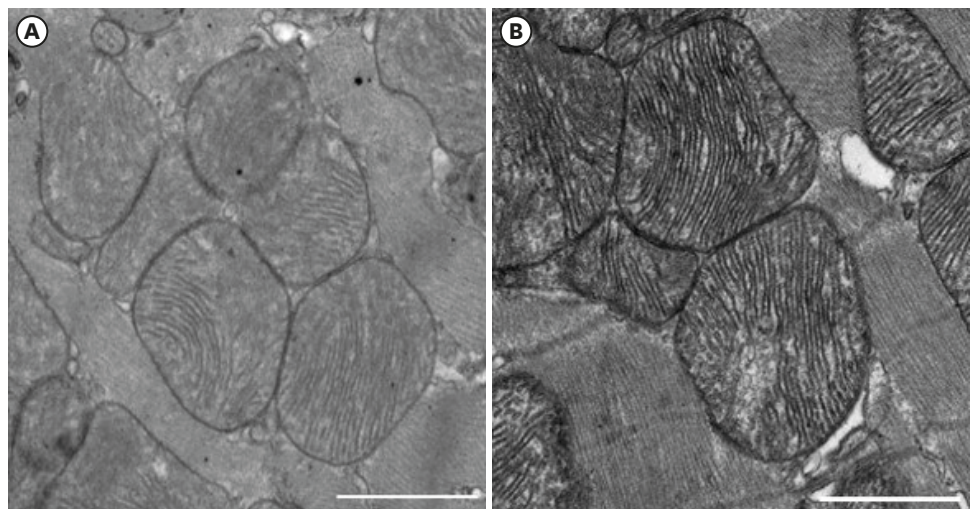


Fig. 2. The electron microscopic image of the mitochondria in the peri-infarction area between AMI and AMI with PF resection. (A) AMI; (B) AMI with PF resection. Transmission electron microscopic images ($\times 3,000$; scale bar 1,000 nm) in the myocardia.

AMI = acute myocardial infarction, PF = pericardial fat.

mRNA expressions of some OXPHOS subunits, antioxidant enzyme and sarcoplasmic reticulum Ca^{2+} ATPase 2 (SERCA2)

Among the genes of complexes I and II implicated in cardiovascular diseases,²⁰ the expressions of OXPHOS in the real-time quantitative RT-PCR showed that the NADH dehydrogenase (ubiquinone) 1 beta subcomplex (NDUFB) 5 was significantly decreased in the AMI group but was significantly recovered in the AMI with PF resection group as previously reported.²¹ However, the expression of NDUFB3, cytochrome c1 (CYC1), NADH dehydrogenase (ubiquinone) flavoprotein 1 (NDUFV1) and NADH dehydrogenase (ubiquinone) Fe-S protein 1 (NDUFS1) were not different between the AMI with PF resection and AMI groups (data not shown). The expression of complex II/succinate dehydrogenase B subunit (SDHB) was also significantly decreased in the AMI group but was recovered in the AMI with PF resection group (Fig. 3). In addition, the expressions of anti-oxidant enzymes such as superoxide dismutase (SOD) and SERCA2 were decreased in the AMI group but were recovered in the AMI with PF resection group (Figs. 3 and 4).

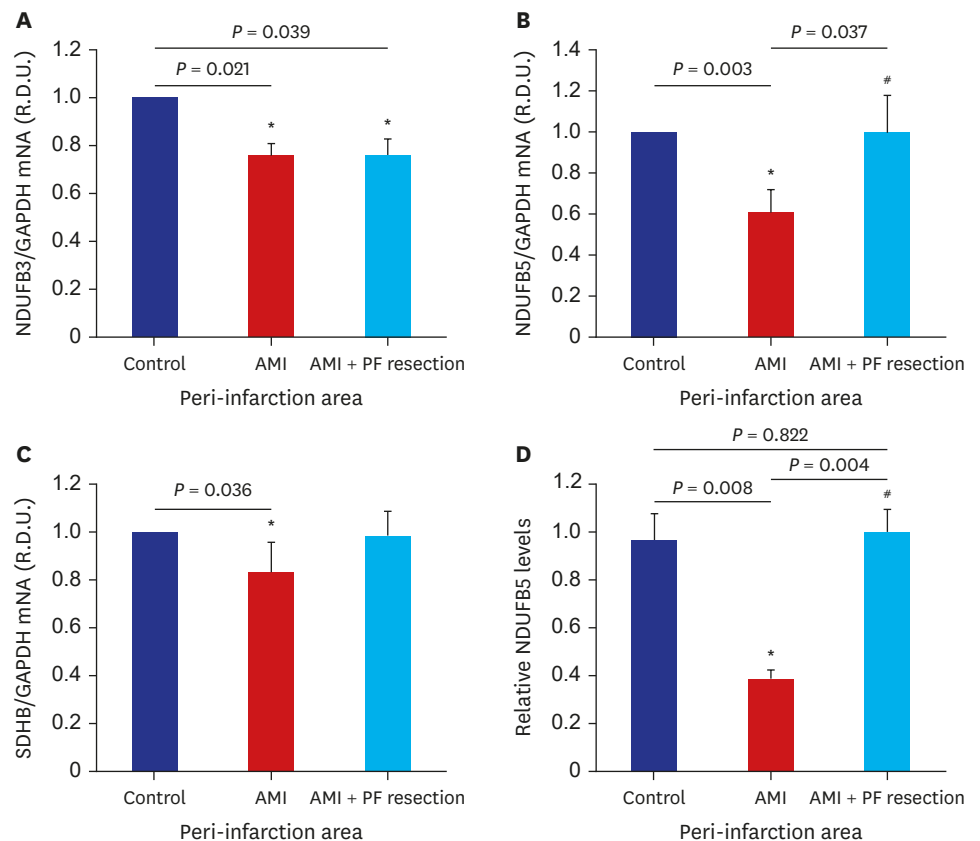


Fig. 3. The comparison of OXPHOS subunit mRNA expression between AMI and AMI with epicardial adipose resection. mRNA expression levels of the following OXPHOS subunits are depicted; NDUFB3 of complex I (A); NDUFB5 of complex I (B); SDHB of complex II (C). Representative blots for OXPHOS subunit: NDUFB5 level (D). Values are expressed as mean ± standard deviation. OXPHOS = oxidative phosphorylation system, AMI = acute myocardial infarction, NDUFB = NADH dehydrogenase (ubiquinone) 1 beta subcomplex, SDHB = succinate dehydrogenase B subunit, PF = pericardial fat. * $P < 0.05$ vs. control; # $P < 0.05$ vs. AMI.

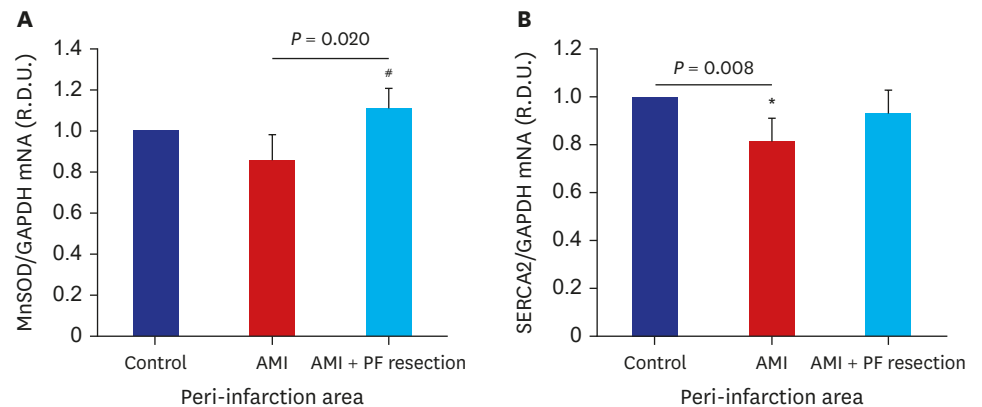


Fig. 4. The comparison of anti-oxidant enzyme and SERCA2 mRNA expression between AMI and AMI with PF resection. **(A)** MnSOD; **(B)** SERCA2. Values are expressed as mean \pm standard deviation.

SERCA2 = sarcoplasmic reticulum Ca^{2+} ATPase 2, AMI = acute myocardial infarction, MnSOD = manganese superoxide dismutase, PF = pericardial fat, GAPDH = glyceraldehyde-3-phosphate dehydrogenase.

* $P < 0.05$ vs. control; # $P < 0.05$ vs. AMI.

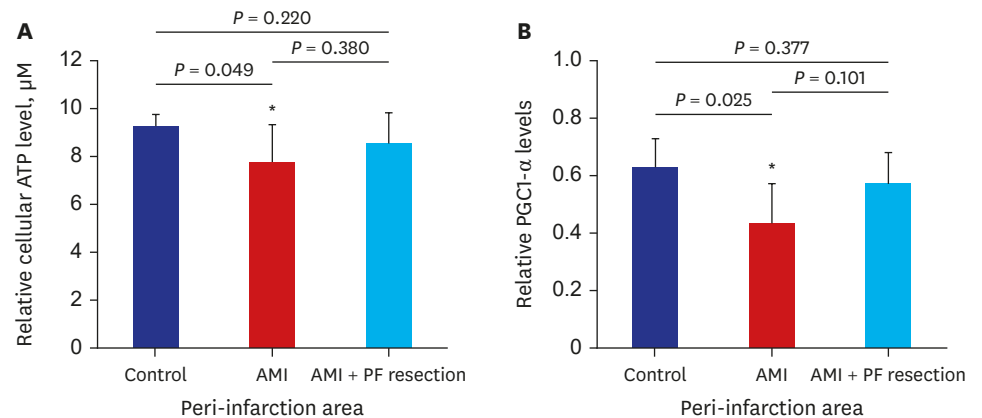


Fig. 5. The comparison of ATP and PGC1- α level in the myocardia between AMI and AMI with pericardial fat resection. **(A)** relative cellular ATP level; **(B)** Representative blots of PGC1- α protein. Values are expressed as mean \pm standard deviation.

ATP = adenosine triphosphate, PGC1- α = peroxisome-proliferator-activated receptor γ , co-activator-1 α , AMI = acute myocardial infarction, PF = pericardial fat.

* $P < 0.05$ vs. control.

ATP and western blot analysis of NDUFB 5 and PGC-1 α

The levels of ATP synthesis were significantly decreased in the AMI group but were recovered in the AMI with PF resection group. PGC-1 α was significantly decreased in the AMI group but was recovered in the AMI with PF resection group (Fig. 5, Supplementary Fig. 2).

DISCUSSION

In the present study, OXPHOS subunit NDUFB5, SDHB and PGC-1 α with ATP were decreased in AMI group but recovered in AMI with PF resection group compared with those in the AMI group. SERCA2 expression and MnSOD were also significantly decreased in AMI group but recovered in AMI with PF resection group compared with those in the AMI group.

A large amount of PF lead to decline release of adiponectin and instead synthesizes proinflammatory adipokines⁶ and the mesenchymal cells from the epicardium could migrate to be transformed into fibroblasts.^{7,8} The accumulation of PF is accompanied by inflammation and fibrosis²²⁻²⁴ and the release of proinflammatory adipocytokines from PF depots may thus contribute to the comorbidities that are characteristically seen in heart failure. Regardless of the source of systemic inflammation, PF itself leads to inflammation and fibrosis of the neighboring myocardium to development of heart failure.²⁵

There is previous report on the relationship between the resection of PF and cardiac dysfunction. The accumulation of PF is also clinically associated with cardiac dysfunction, and structural remodeling in obese people,^{26,27} and surgical resection for PF in AMI could induce beneficial effects for ischemic heart disease.⁹⁻¹¹

Mitochondria have been found to play an important role in the cardiac energetics in the energy production of ATP²⁸ and mitochondria occupy 30–40% of the total area of a cardiomyocyte, where it is indispensable for normal cardiac energetics.^{29,30} The ob/ob and db/db mice and fa/fa rats with systolic dysfunction which show a decreased rate of intracellular Ca²⁺ reduction via SERCA2 in myocytes.³¹⁻³⁶ Mitochondria are also responsible to maintain intracellular Ca²⁺ turnover and the constant energy demands by oxidative phosphorylation (gene set as OXPHOS), and decreased calcium handling was found in the heart failure.^{37,38} In addition, mitochondrial genes such as OXPHOS and PGC1- α , a key metabolic regulator that coordinates in mitochondrial biogenesis^{13,21} and PGC1- α also acts as a crucial regulator of oxidative metabolism in cardiovascular disease. PGC1- α -null mice develop heart failure due to reduced mitochondrial OXPHOS in myocardial energy metabolism³⁹ and oxidative stress has been known to be another axis in heart failure, and deficiencies of anti-oxidant enzyme contribute to mitochondrial damage in AMI^{40,41} as well.

In the present study, the myocardial mitochondria in the AMI with PF resection group showed more electro-dense cristae and membrane than those in the AMI group. The mitochondrial outer membrane has specific components for communication with other intra-cellular organelles and for the recognition and import of mitochondrial proteins while the inner membrane, the tubular-like cristae is the main machinery for respiratory chain complex containing OXPHOS for oxidative phosphorylation in the form of ATP. In our present study, it is speculated that more electro-dense crista might be related to more respiratory capacity in the mitochondria energy metabolism in the PF resection group.⁴² The expression of SERCA2 was recovered in the AMI with PF resection group compared with that in the AMI group, and the expressions of the OXPHOS subunit NDUFB5, SDHB, anti-oxidant enzyme and PGC-1 α were also recovered in the AMI with PF resection group compared with those in the AMI group which were subsequently associated with increased ATP levels. Improved mitochondrial ATP synthesis in the non-infarct area might be related to increased systolic function in the AMI with PF resection group. However, further basic study is needed to support the beneficial effect for improvement of cardiac systolic function in the resection of PF.

There are some limitations in this study. First, this study included a relatively small number of animals which may limit the generalization of the results. Second, the volume and area of resected PF could be dependent on the operator and cardiac anatomy. Especially, pericardial or epicardial fat in the small animal was indistinguishable during the AMI operation. Third, a more detailed targeted experiment is needed to investigate the relationship between PF

resection and the improvement of cardiac systolic function. Forth, the experiment was a prospective study, but unmeasured selection bias may exist. Collectively, PF resection might be a beneficial effect to ameliorate myocardial mitochondrial dysfunction in the obese AMI rat model.

In conclusion, even though the myocardial mitochondrial morphology in the non-infarction area seemed to be similar between the AMI and AMI with PF resection groups, AMI with PF resection showed improved expressions of PGC-1 α , antioxidant enzyme and OXPHOS subunit associated with ATP synthesis compared to AMI. Therefore, surgical resection of PF in the obese AMI might ameliorate myocardial mitochondria dysfunction.

SUPPLEMENTARY MATERIALS

Supplementary Table 1

Primer sequences of real-time polymerase chain reaction

[Click here to view](#)

Supplementary Fig. 1

Study design and comparison of weight gain between AMI and AMI with PF resection. Data are expressed as mean \pm standard error (n = 7).

[Click here to view](#)

Supplementary Fig. 2

The example for comparison of western blot analysis of NDUFB5 and PGC-1 α between AMI and AMI with PF resection. (A) NDUFB5 level; (B) PGC1- α level.

[Click here to view](#)

REFERENCES

1. Ruan Y, Guo Y, Zheng Y, Huang Z, Sun S, Kowal P, et al. Cardiovascular disease (CVD) and associated risk factors among older adults in six low-and middle-income countries: results from SAGE Wave 1. *BMC Public Health* 2018;18(1):778.
[PUBMED](#) | [CROSSREF](#)
2. Song DK, Hong YS, Lee H, Oh JY, Sung YA, Kim Y. Increased epicardial adipose tissue thickness in type 2 diabetes mellitus and obesity. *Diabetes Metab J* 2015;39(5):405-13.
[PUBMED](#) | [CROSSREF](#)
3. Bentley-Lewis R, Adler GK, Perlstein T, Seely EW, Hopkins PN, Williams GH, et al. Body mass index predicts aldosterone production in normotensive adults on a high-salt diet. *J Clin Endocrinol Metab* 2007;92(11):4472-5.
[PUBMED](#) | [CROSSREF](#)
4. Kenchaiah S, Evans JC, Levy D, Wilson PW, Benjamin EJ, Larson MG, et al. Obesity and the risk of heart failure. *N Engl J Med* 2002;347(5):305-13.
[PUBMED](#) | [CROSSREF](#)
5. Shin SY, Yong HS, Lim HE, Na JO, Choi CU, Choi JI, et al. Total and interatrial epicardial adipose tissues are independently associated with left atrial remodeling in patients with atrial fibrillation. *J Cardiovasc Electrophysiol* 2011;22(6):647-55.
[PUBMED](#) | [CROSSREF](#)

6. Bambace C, Sepe A, Zoico E, Telesca M, Oliosio D, Venturi S, et al. Inflammatory profile in subcutaneous and epicardial adipose tissue in men with and without diabetes. *Heart Vessels* 2014;29(1):42-8.
[PUBMED](#) | [CROSSREF](#)
7. Naftali-Shani N, Levin-Kotler LP, Palevski D, Amit U, Kain D, Landa N, et al. Left ventricular dysfunction switches mesenchymal stromal cells toward an inflammatory phenotype and impairs their reparative properties via Toll-like receptor-4. *Circulation* 2017;135(23):2271-87.
[PUBMED](#) | [CROSSREF](#)
8. Ruiz-Villalba A, Simón AM, Pogontke C, Castillo MI, Abizanda G, Pelacho B, et al. Interacting resident epicardium-derived fibroblasts and recruited bone marrow cells form myocardial infarction scar. *J Am Coll Cardiol* 2015;65(19):2057-66.
[PUBMED](#) | [CROSSREF](#)
9. McKenney-Drake ML, Rodenbeck SD, Bruning RS, Kole A, Yancey KW, Alloosh M, et al. Epicardial adipose tissue removal potentiates outward remodeling and arrests coronary atherogenesis. *Ann Thorac Surg* 2017;103(5):1622-30.
[PUBMED](#) | [CROSSREF](#)
10. Chang HX, Zhao XJ, Zhu QL, Hou Q, Li Y. Removal of epicardial adipose tissue after myocardial infarction improves cardiac function. *Herz* 2018;43(3):258-64.
[PUBMED](#) | [CROSSREF](#)
11. Bière L, Behaghel V, Mateus V, Assunção A Jr, Gräni C, Ouerghi K, et al. Relation of quantity of subepicardial adipose tissue to infarct size in patients with ST-elevation myocardial infarction. *Am J Cardiol* 2017;119(12):1972-8.
[PUBMED](#) | [CROSSREF](#)
12. Johannsen DL, Ravussin E. The role of mitochondria in health and disease. *Curr Opin Pharmacol* 2009;9(6):780-6.
[PUBMED](#) | [CROSSREF](#)
13. Kang KW, Kim OS, Chin JY, Kim WH, Park SH, Choi YJ, et al. Diastolic dysfunction induced by a high-fat diet is associated with mitochondrial abnormality and adenosine triphosphate levels in rats. *Endocrinol Metab (Seoul)* 2015;30(4):557-68.
[PUBMED](#) | [CROSSREF](#)
14. Zhu N, Yan X, Li H, Wang H. Clinical significance of serum PGC-1 alpha levels in diabetes mellitus with myocardial infarction patients and reduced ROS-oxidative stress in diabetes mellitus with myocardial infarction model. *Diabetes Metab Syndr Obes* 2020;13:4041-9.
[PUBMED](#) | [CROSSREF](#)
15. Singh SP, Schragenheim J, Cao J, Falck JR, Abraham NG, Bellner L. PGC-1 alpha regulates HO-1 expression, mitochondrial dynamics and biogenesis: role of epoxyeicosatrienoic acid. *Prostaglandins Other Lipid Mediat* 2016;125:8-18.
[PUBMED](#) | [CROSSREF](#)
16. Wojtovich AP, Smith CO, Haynes CM, Nehrke KW, Brookes PS. Physiological consequences of complex II inhibition for aging, disease, and the mKATP channel. *Biochim Biophys Acta* 2013;1827(5):598-611.
[PUBMED](#) | [CROSSREF](#)
17. Matsubara LS, Matsubara BB, Okoshi MP, Cicogna AC, Janicki JS. Alterations in myocardial collagen content affect rat papillary muscle function. *Am J Physiol Heart Circ Physiol* 2000;279(4):H1534-9.
[PUBMED](#) | [CROSSREF](#)
18. Heaps CL, Tharp DL, Bowles DK. Hypercholesterolemia abolishes voltage-dependent K⁺ channel contribution to adenosine-mediated relaxation in porcine coronary arterioles. *Am J Physiol Heart Circ Physiol* 2005;288(2):H568-76.
[PUBMED](#) | [CROSSREF](#)
19. Sahn DJ, DeMaria A, Kisslo J, Weyman A. Recommendations regarding quantitation in M-mode echocardiography: results of a survey of echocardiographic measurements. *Circulation* 1978;58(6):1072-83.
[PUBMED](#) | [CROSSREF](#)
20. Sparks LM, Xie H, Koza RA, Mynatt R, Hulver MW, Bray GA, et al. A high-fat diet coordinately downregulates genes required for mitochondrial oxidative phosphorylation in skeletal muscle. *Diabetes* 2005;54(7):1926-33.
[PUBMED](#) | [CROSSREF](#)
21. Mootha VK, Lindgren CM, Eriksson KF, Subramanian A, Sihag S, Lehar J, et al. PGC-1alpha-responsive genes involved in oxidative phosphorylation are coordinately downregulated in human diabetes. *Nat Genet* 2003;34(3):267-73.
[PUBMED](#) | [CROSSREF](#)

22. Nakanishi K, Fukuda S, Tanaka A, Otsuka K, Taguchi H, Yoshikawa J, et al. Epicardial adipose tissue accumulation is associated with renal dysfunction and coronary plaque morphology on multidetector computed tomography. *Circ J* 2016;80(1):196-201.
[PUBMED](#) | [CROSSREF](#)
23. Patel VB, Mori J, McLean BA, Basu R, Das SK, Ramprasath T, et al. ACE2 deficiency worsens epicardial adipose tissue inflammation and cardiac dysfunction in response to diet-induced obesity. *Diabetes* 2016;65(1):85-95.
[PUBMED](#) | [CROSSREF](#)
24. Packer M. Leptin-aldosterone-nephrilysin axis: identification of its distinctive role in the pathogenesis of the three phenotypes of heart failure in people with obesity. *Circulation* 2018;137(15):1614-31.
[PUBMED](#) | [CROSSREF](#)
25. Patel VB, Shah S, Verma S, Oudit GY. Epicardial adipose tissue as a metabolic transducer: role in heart failure and coronary artery disease. *Heart Fail Rev* 2017;22(6):889-902.
[PUBMED](#) | [CROSSREF](#)
26. Wu CK, Tsai HY, Su MM, Wu YF, Hwang JJ, Lin JL, et al. Evolutional change in epicardial fat and its correlation with myocardial diffuse fibrosis in heart failure patients. *J Clin Lipidol* 2017;11(6):1421-31.
[PUBMED](#) | [CROSSREF](#)
27. Iacobellis G, Leonetti F, Singh N, M Sharma A. Relationship of epicardial adipose tissue with atrial dimensions and diastolic function in morbidly obese subjects. *Int J Cardiol* 2007;115(2):272-3.
[PUBMED](#) | [CROSSREF](#)
28. Parra V, Verdejo H, del Campo A, Pennanen C, Kuzmich J, Iglewski M, et al. The complex interplay between mitochondrial dynamics and cardiac metabolism. *J Bioenerg Biomembr* 2011;43(1):47-51.
[PUBMED](#) | [CROSSREF](#)
29. Rasola A, Bernardi P. The mitochondrial permeability transition pore and its involvement in cell death and in disease pathogenesis. *Apoptosis* 2007;12(5):815-33.
[PUBMED](#) | [CROSSREF](#)
30. Javadov S, Karmazyn M. Mitochondrial permeability transition pore opening as an endpoint to initiate cell death and as a putative target for cardioprotection. *Cell Physiol Biochem* 2007;20(1-4):1-22.
[PUBMED](#) | [CROSSREF](#)
31. Li SY, Yang X, Ceylan-Isik AF, Du M, Sreejayan N, Ren J. Cardiac contractile dysfunction in Lep/Lep obesity is accompanied by NADPH oxidase activation, oxidative modification of sarco(endo)plasmic reticulum Ca²⁺-ATPase and myosin heavy chain isozyme switch. *Diabetologia* 2006;49(6):1434-46.
[PUBMED](#) | [CROSSREF](#)
32. Dong F, Zhang X, Yang X, Esberg LB, Yang H, Zhang Z, et al. Impaired cardiac contractile function in ventricular myocytes from leptin-deficient ob/ob obese mice. *J Endocrinol* 2006;188(1):25-36.
[PUBMED](#) | [CROSSREF](#)
33. Ren J, Dong F, Cai GJ, Zhao P, Nunn JM, Wold LE, et al. Interaction between age and obesity on cardiomyocyte contractile function: role of leptin and stress signaling. *PLoS One* 2010;5(4):e10085.
[PUBMED](#) | [CROSSREF](#)
34. Dong F, Zhang X, Ren J. Leptin regulates cardiomyocyte contractile function through endothelin-1 receptor-NADPH oxidase pathway. *Hypertension* 2006;47(2):222-9.
[PUBMED](#) | [CROSSREF](#)
35. Minhas KM, Khan SA, Raju SV, Phan AC, Gonzalez DR, Skaf MW, et al. Leptin repletion restores depressed beta-adrenergic contractility in ob/ob mice independently of cardiac hypertrophy. *J Physiol* 2005;565(Pt 2):463-74.
[PUBMED](#) | [CROSSREF](#)
36. Ren J, Sowers JR, Walsh MF, Brown RA. Reduced contractile response to insulin and IGF-I in ventricular myocytes from genetically obese Zucker rats. *Am J Physiol Heart Circ Physiol* 2000;279(4):H1708-14.
[PUBMED](#) | [CROSSREF](#)
37. Bugger H, Abel ED. Mitochondria in the diabetic heart. *Cardiovasc Res* 2010;88(2):229-40.
[PUBMED](#) | [CROSSREF](#)
38. Bers DM, Shannon TR. Calcium movements inside the sarcoplasmic reticulum of cardiac myocytes. *J Mol Cell Cardiol* 2013;58:59-66.
[PUBMED](#) | [CROSSREF](#)
39. Finck BN, Kelly DP. PGC-1 coactivators: inducible regulators of energy metabolism in health and disease. *J Clin Invest* 2006;116(3):615-22.
[PUBMED](#) | [CROSSREF](#)
40. Furukawa S, Fujita T, Shimabukuro M, Iwaki M, Yamada Y, Nakajima Y, et al. Increased oxidative stress in obesity and its impact on metabolic syndrome. *J Clin Invest* 2004;114(12):1752-61.
[PUBMED](#) | [CROSSREF](#)

41. Marí M, Morales A, Colell A, García-Ruiz C, Fernández-Checa JC. Mitochondrial glutathione, a key survival antioxidant. *Antioxid Redox Signal* 2009;11(11):2685-700.
[PUBMED](#) | [CROSSREF](#)
42. Quintana-Cabrera R, Mehrotra A, Rigoni G, Soriano ME. Who and how in the regulation of mitochondrial cristae shape and function. *Biochem Biophys Res Commun* 2018;500(1):94-101.
[PUBMED](#) | [CROSSREF](#)